Comparison of Semiempirical and ab Initio Transition States

Stefan Schröder and Walter Thiel*

Contribution from Theoretische Chemie, Bergische Universität—Gesamthochschule Wuppertal, D-5600 Wuppertal 1, West Germany. Received December 5, 1984

Abstract: MNDO and MNDOC calculations are reported for 24 reactions of simple organic molecules. The results are compared with those from state-of-the-art ab initio calculations. Satisfactory agreement is generally found for the geometries, frequencies, and zero-point vibrational energies of transition states. The ab initio activation energies are reproduced more closely by MNDOC than by MNDO. The comparisons clarify the accuracy which may be expected in semiempirical calculations of transition states and thereby allow a more detailed justification for applying MNDO and MNDOC to the study of chemical reactions.

1. Introduction

There are several semiempirical methods[1-5] which have been designed for calculating potential surfaces of large molecules, e.g., MNDO[3] and its correlated version MNDOC.[5] For stable molecules, the reliability of these methods has been established by systematic comparisons with experimental data so that mean absolute errors are available for many ground-state properties.[3-7] For transition states, such systematic tests have not been feasible due to the lack of experimental data, e.g., for transition-state geometries. As a consequence, semiempirical predictions for transition states have sometimes been met with scepticism based on the feeling that they merely represent uncertain extrapolations on potential surfaces.

In view of the widespread use of semiempirical methods for computing chemical reactions (see, e.g., ref 8–10 for an incomplete list of recent MNDO applications), it is clearly desirable to establish their reliability in this connection more securely. In the absence of sufficient experimental data, this can only be done by comparing the semiempirical results with those from elaborate ab initio calculations. Fortunately, during the last 5 years (i.e., after the publication of MNDO[3] and the development of MNDOC[5]), ab initio transition structures have become available which have been fully optimized by analytical gradient techniques. These structures and the corresponding energies from state-of-the-art ab initio treatments are not exact, of course, but they are considered reliable enough to serve as reference data for our purposes.

The present paper provides a systematic evaluation of MNDO and MNDOC calculations for transition states. Comparisons with

(1) Pople, J. A.; Segal, G. A. J. Chem. Phys. 1966, 44, 3289.

(2) Bingham, R. C.; Dewar, M. J. S.; Lo, D. H. J. Am. Chem. Soc. 1975, 97, 1285.

(3) Dewar, M. J. S.; Thiel, W. J. Am. Chem. Soc. 1977, 99, 4899, 4907.

(4) Nanda, D. N.; Jug, K. Theor. Chim. Acta 1980, 57, 95. Jug, K.; Nanda, D. N. Theor. Chim. Acta 1980, 57, 107, 131.

(5) Thiel, W. J. Am. Chem. Soc. 1981, 103, 1413.

(6) Dewar, M. J. S.; Rzepa, H. S. J. Am. Chem. Soc. 1978, 100, 784.

(7) Dewar, M. J. S.; Ford, G. P.; McKee, M. L.; Rzepa, H. S.; Thiel, W.; Yamaguchi, Y. J. Mol. Struct. 1978, 43, 135.

(8) Ford, G. P.; Scribner, J. D. J. Am. Chem. Soc. 1983, 105, 349. Storch, D. M.; Dymek, C. J., Jr.; Davis, L. P. J. Am. Chem. Soc. 1983, 105, 1765. Apeloig, Y.; Ciommer, B.; Frenking, G.; Karni, M.; Mandelbaum, A.; Schwarz, H.; Weisz, A. J. Am. Chem. Soc. 1983, 105, 2186. Apeloig, Y.; Karni, M.; Stang, P. J.; Fox, D. P. J. Am. Chem. Soc. 1983, 105, 4781. Dewar, M. J. S.; Chantrapunong, L. J. Am. Chem. Soc. 1983, 105, 7152, 7161. Rayez, J. C.; Rayez, M. T.; Duguay, B. J. Chem. Phys. 1983, 78, 827. Engelke, R.; Hay, P. J.; Kleier, D. A.; Wadt, W. R. J. Chem. Phys. 1983, 79, 4367. Dormans, G. J. M.; Fransen, H. R.; Buck, H. M. J. Am. Chem. Soc. 1984, 106, 1213. Carrion, F.; Dewar, M. J. S. J. Am. Chem. Soc. 1984, 106, 3531. Dewar, M. J. S.; Kuhn, D. R. J. Am. Chem. Soc. 1984, 106, 5256. Engelke, R.; Hay, P. J.; Kleier, D. A.; Wadt, W. R. J. Am. Chem. Soc. 1984, 106, 5439. Turner, A. G.; Davis, L. P. J. Am. Chem. Soc. 1984, 106, 5447. Bock, H.; Roth, B.; Maier, G. Chem. Ber. 1984, 117, 172. Lebrilla, C. B.; Maier, W. F. Chem. Phys. Lett. 1984, 105, 183. Frenking, G.; Heinrich, N.; Koch, W.; Schwarz, H. Chem. Phys. Lett. 1984, 105, 490. Frenking, G.; Schmidt, J. Tetrahedron 1984, 40, 2123.

(9) Shea, J. P.; Nelson, S. D.; Ford, G. P. J. Am. Chem. Soc. 1983, 105, 5451. Pudzianowski, A. T.; Loew, G. H.; Mico, B. A.; Blanchflower, R. V.; Pohl, L. R. J. Am. Chem. Soc. 1983, 105, 3434. Pudzianowski, A. T.; Loew, G. H. J. Phys. Chem. 1983, 87, 1081. Pudzianowski, A. T.; Loew, G. H. Int. J. Quant. Chem. 1983, 23, 1257.

(10) Barone, V.; Bianchi, N.; Lelj, F. Chem. Phys. Lett. 1983, 98, 463.

Scheme I
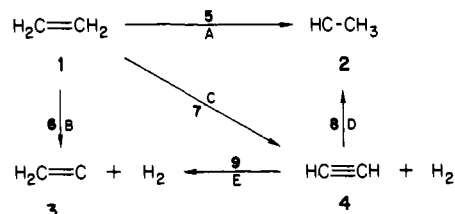
Scheme II
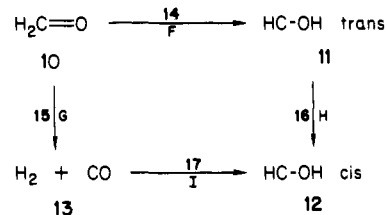
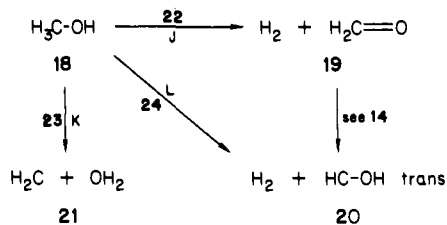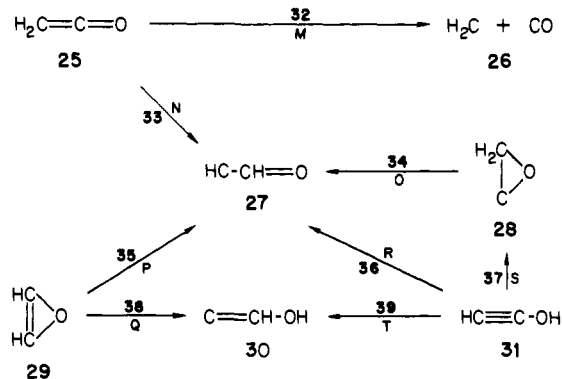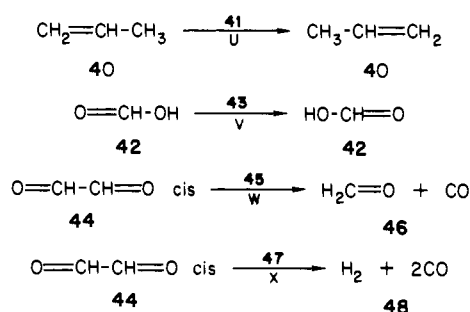**Scheme III**

Scheme IV

ab initio reference calculations are carried out for a set of 24 reactions of small organic molecules, with regard to transition structures, activation energies, zero-point vibrational energies, and transition-state frequencies.

2. Ab Initio Reference Data

The selection of ab initio reference data from published material is based on the following guidelines.

Scheme V

$$CH_2\!=\!CH\text{-}CH_3 \xrightarrow[U]{41} CH_3\text{-}CH\!=\!CH_2$$
$$\textbf{40} \qquad\qquad\qquad \textbf{40}$$

$$O\!=\!CH\text{-}OH \xrightarrow[V]{43} HO\text{-}CH\!=\!O$$
$$\textbf{42} \qquad\qquad\qquad \textbf{42}$$

$$O\!=\!CH\text{-}CH\!=\!O \text{ cis} \xrightarrow[W]{45} H_2C\!=\!O + CO$$
$$\textbf{44} \qquad\qquad\qquad\qquad \textbf{46}$$

$$O\!=\!CH\text{-}CH\!=\!O \text{ cis} \xrightarrow[X]{47} H_2 + 2CO$$
$$\textbf{44} \qquad\qquad\qquad\qquad \textbf{48}$$

(a) Transition structures are required to be fully optimized by gradient techniques and characterized by force constant analysis.

(b) Geometry optimizations at the restricted Hartree–Fock (RHF) level must involve a basis set of at least split-valence quality. To be as consistent as possible, we accept only the standard basis sets developed by the Pople group, e.g., 3-21G,[11] 4-31G,[12] and 6-31G*.[13]

(c) Geometry optimizations at the correlated level are not included since we wish to compare semiempirical and ab initio RHF transition structures. The correlation effects on such structures are often fairly small, anyway (see, e.g., ref 16).

(d) For all RHF-optimized transition structures, high-level energy calculations must be available which make use of basis sets with polarization functions and a suitable correlation treatment.

(e) The reference systems must consist of the elements H,C,N, and O since MNDOC, unlike MNDO, has only been parametrized for these elements.

Following these guidelines, we have selected ab initio reference calculations which deal with the potential surfaces of ethylene,[14,15] formaldehyde,[15–17] methanol,[15,16] ketene,[18] propene,[19] formic acid,[19] and *cis*-glyoxal.[20] In addition to these reference calculations,[14–20] there are a number of other ab initio studies on these systems,[21–29] some of which are discussed below (see section 4). Schemes I–V show the investigated reactions which are denoted by capital letters whereas the minima and transition states involved are identified by boldface numbers. The selected set of 24 reactions includes six [1,2]- and two [1,3]-sigmatropic hydrogen shifts, five other

Figure 1. Definition of transition structures.

Figure 2. Planar transition structures drawn to scale. The solid lines show the optimized ab initio RHF geometries (defined as in Figure 1) while the crosses mark the positions of the atoms in MNDOC.

intramolecular rearrangements, four 1,1 and three 1,2 eliminations of H_2, and four other dissociation reactions.

3. Semiempirical Calculations

The MNDO and MNDOC calculations were carried out by using standard parameters[3,5] and programs.[30,31] All geometries were optimized at the SCF level by employing the Davidon–Fletcher–Powell algorithm[32] for minima and gradient norm minimization[33,34] for transition states. In most cases, the automatic optimization program was successful in locating transition structures when starting the search at the corresponding published ab initio structure; if not, suitable starting points were found by the usual reaction coordinate or grid search techniques. Energies were evaluated at the MNDO SCF level[3] and the correlated MNDOC BWEN level[5] as recommended.[35] A force constant analysis was performed for all MNDO SCF stationary points.

4. Results

The transition structures are defined in Figure 1 and Table I. Figure 2 allows a visual comparison between the MNDOC and ab initio RHF geometries of all planar transition states studied. Tables II and III list relative energies for the species **1–39** obtained from MNDO and MNDOC heats of formation and from ab initio

(11) Binkley, J. S.; Pople, J. A.; Hehre, W. J. *J. Am. Chem. Soc.* **1980**, *102*, 939.

(12) Ditchfield, R.; Hehre, W. J.; Pople, J. A. *J. Chem. Phys.* **1971**, *54*, 724.

(13) Hariharan, P. C.; Pople, J. A. *Chem. Phys. Lett.* **1972**, *16*, 217.

(14) Raghavachari, K.; Frisch, M. J.; Pople, J. A.; Schleyer, P. v. R. *Chem. Phys. Lett.* **1982**, *85*, 145.

(15) Whiteside, R. A.; Binkley, J. S.; Krishnan, R.; DeFrees, D. J.; Schlegel, H. B.; Pople, J. A. "Carnegie-Mellon Quantum Chemistry Archive"; Carnegie-Mellon University: Pittsburgh, 1980.

(16) Harding, L. B.; Schlegel, H. B.; Krishnan, R.; Pople, J. A. *J. Phys. Chem.* **1980**, *84*, 3394.

(17) Frisch, M. J.; Binkley, J. S.; Schaefer, H. F., III. *J. Chem. Phys.* **1984**, *81*, 1882.

(18) Bouma, W. J.; Nobes, R. H.; Radom, L.; Woodward, C. E. *J. Org. Chem.* **1982**, *47*, 1869.

(19) Rodwell, W. R.; Bouma, W. J.; Radom, L. *Int. J. Quant. Chem.* **1980**, *23*, 107.

(20) Osamura, Y.; Schaefer, H. F., III; Dupuis, M.; Lester, W. A., Jr. *J. Chem. Phys.* **1981**, *75*, 5828.

(21) Nobes, R. H.; Radom, L.; Rodwell, W. R. *Chem. Phys. Lett.* **1980**, *74*, 269.

(22) Goddard, J. D.; Schaefer, H. F., III. *J. Chem. Phys.* **1979**, *70*, 5117.

(23) Goddard, J. D.; Yamaguchi, Y.; Schaefer, H. F., III. *J. Chem. Phys.* **1981**, *75*, 3459.

(24) Adams, G. F.; Bent, G. D.; Bartlett, R. J.; Purvis, G. D. *J. Chem. Phys.* **1981**, *75*, 834.

(25) Frisch, M. J.; Krishnan, R.; Pople, J. A. *J. Phys. Chem.* **1981**, *85*, 1467.

(26) Dupuis, M.; Lester, W. A., Jr.; Lengsfield, B. H., III. Liu, B. *J. Chem. Phys.* **1983**, *79*, 6167.

(27) Tanaka, K.; Yoshimine, M. *J. Am. Chem. Soc.* **1980**, *102*, 7655.

(28) Bernardi, F.; Robb, M. A.; Schlegel, H. B.; Tanachini, G. *J. Am. Chem. Soc.* **1984**, *106*, 1198.

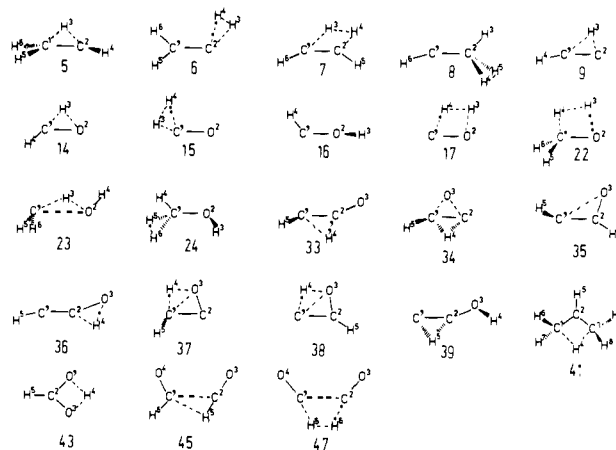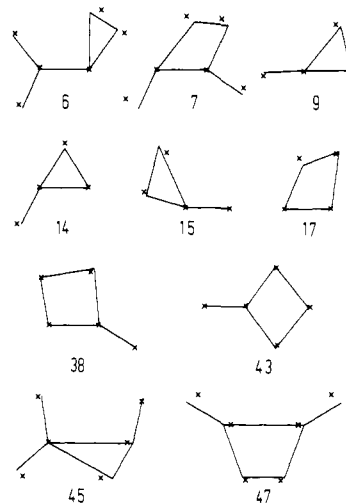(29) For earlier ab initio studies, see citations in ref 14, 16–28.

(30) Thiel, W. In "Quantum Chemistry Program Exchange Catalog"; Indiana University: Bloomington, 1982; Vol. 14, program 438.

(31) Routines for the location of transition states and for force constant analysis are available, e.g., from MOPAC: Stewart, J. P. In "Quantum Chemistry Program Exchange Catalog"; Indiana University: Bloomington, 1983; Vol. 15, program 455.

(32) Fletcher, R.; Powell, M. J. D. *Comput. J.* **1963**, *6*, 163. Davidon, W. C. *Comput. J.* **1968**, *10*, 406.

(33) McIver, J. W., Jr.; Komornicki, A. *J. Am. Chem. Soc.* **1972**, *94*, 2625.

(34) Weiner, P. K. Ph.D. Thesis, University of Texas, Austin, 1975.

(35) Thiel, W. *J. Am. Chem. Soc.* **1981**, *103*, 1420.

Table I. Comparison of SCF-Optimized Transition Structures[a]

system	point group	variable[b,c]	MNDO	MNDOC	ab initio[d,e]	ref
5	C_1	C^1C^2	1.378	1.397	1.378	*f*
		C^1H^3	1.320	1.364	1.325	
		C^2H^3	1.402	1.321	1.266	
		C^2H^4	1.072	1.103	1.088	
		C^1H^5	1.099	1.096	1.081	
		C^1H^6	1.100	1.098	1.086	
		$H^4C^2C^1$	130.7	113.0	108.9	
		$H^5C^1C^2$	121.5	120.4	119.9	
		$H^6C^1C^2$	124.2	127.5	126.1	
		$H^4C^2C^1H^3$	101.8	100.7	100.7	
		$H^5C^1C^2H^3$	88.1	84.8	76.5	
		$H^6C^1C^2H^3$	−113.9	−109.1	−107.5	
6	C_s	C^1C^2	1.319	1.313	1.322	*g*
		C^2H^3	1.284	1.253	1.249	
		C^2H^4	1.682	1.507	1.461	
		H^3H^4	0.813	0.836	0.838	
		C^1H^5	1.091	1.090	*h*	
		C^1H^6	1.089	1.089	*h*	
		$H^3C^2C^1$	135.3	136.0	126.4	
		$H^5C^1C^2$	119.5	117.9	114.3	
		$H^6C^1C^2$	127.0	128.9	130.1	
7	C_s	C^1C^2	1.271	1.275	1.323	*g*
		C^1H^3	1.563	1.542	1.557	
		C^2H^3	1.367	1.419	1.265	
		C^2H^4	1.370	1.384	1.272	
		H^3H^4	0.985	0.919	0.886	
		C^2H^5	1.076	1.081	*h*	
		C^1H^6	1.051	1.072	*h*	
		$H^5C^2C^1$	148.0	157.1	147.2	*i*
		$H^6C^1C^2$	160.9	136.2	115.5	*i*
8	C_s	C^1C^2	1.281	1.264	1.308	*g*
		C^2H^3	1.090	1.096	*h*	
		C^2H^4	1.285	1.265	1.374	
		H^4H^5	1.007	1.040	0.829	
		C^1H^6	1.048	1.054	*h*	
		$H^3C^2C^1$	132.4	134.4	139.3	
		$H^6C^1C^2$	165.5	178.6	118.5	
		$C^1–C^2H^4H^5$	121.4	120.5	*h*	
9	C_s	C^1C^2	1.270	1.261	1.237	*f*
		C^1H^3	1.371	1.402	1.459	
		C^2H^3	1.322	1.269	1.170	
		C^1H^4	1.059	1.067	1.062	
		$H^4C^1C^2$	167.0	172.7	180.4	
14	C_s	C^1O^2	1.283	1.260	1.270	*j*
		C^1H^3	1.303	1.280	1.219	
		O^2H^3	1.247	1.278	1.175	
		C^1H^4	1.098	1.112	1.095	
		$H^4C^1O^2$	121.4	119.5	115.9	
15	C_s	C^1O^2	1.180	1.168	1.134	*j,k*
		C^1H^3	1.142	1.147	1.094	
		C^1H^4	1.531	1.433	1.739	
		H^3H^4	1.060	1.080	1.328	
		$H^3C^1O^2$	157.2	159.3	164.5	
		$H^4C^1O^2$	113.4	111.3	114.7	
16	C_1	C^1O^2	1.328	1.314	1.347	*j*
		O^2H^3	0.942	0.929	0.951	
		C^1H^4	1.127	1.137	1.109	
		$H^3O^2C^1$	120.8	119.5	115.2	
		$H^4C^1O^2$	110.6	108.5	104.9	
		$H^3O^2C^1H^4$	91.5	91.3	90.1	
17	C_s	C^1O^2	1.255	1.240	1.231	*f*
		O^2H^3	1.470	1.412	1.482	
		C^1H^4	1.293	1.292	1.169	
		H^3H^4	1.058	1.039	1.112	
		$H^3O^2C^1$	92.7	96.0	97.0	
		$H^4C^1O^2$	77.2	73.8	72.1	
22	C_s	C^1O^3	1.313	1.299	1.310	*j*
		O^2H^3	1.451	1.447	1.385	
		C^1H^4	1.406	1.394	1.408	
		H^3H^4	0.995	0.984	0.947	
		C^1H^5	1.114	1.115	1.087[*f*]	

Table I (Continued)

system	point group	variable[b,c]	MNDO	MNDOC	ab initio[d,e]	ref
22	C_s	$H^3O^2C^1$	63.7	62.3	57.5	j
		$H^4C^1O^2$	103.2	104.8	105.3	
		$H^5C^1O^2$	119.3	120.1	119.8	
		$H^5C^1O^2H^3$	108.7	107.8	106.0	
23	C_1	C^1O^2	1.897	1.816	1.806	j, l
		C^1H^3	1.196	1.222	1.308	
		O^2H^3	1.196	1.216	1.116	
		O^2H^4	0.941	0.930	0.951	
		C^1H^5	1.091	1.100	1.077	
		C^1H^6	1.091	1.100	1.080	
		$H^4O^2H^3$	98.1	93.0	107.0	
		$H^5C^1H^6$	114.0	108.5	110.8	
		H^5C^1M	108.5	107.5	108.3	m
		H^6C^1M	108.5	107.5	108.3	m
24	C_1	C^1O^2	1.327	1.325	1.347	j
		O^2H^3	0.951	0.938	0.947	
		C^1H^4	1.097	1.111	1.084	
		C^1H^5	1.660	1.533	1.574	
		C^1H^6	1.289	1.262	1.298	
		H^5H^6	0.859	0.882	0.852	
		$H^3O^2C^1$	112.0	109.8	108.6	
		$H^4C^1O^2$	113.9	110.4	109.1	
		$H^5C^1H^4$	95.4	90.4	83.4	
		$H^6C^1H^4$	112.1	111.5	106.6	
		$H^5C^1H^6$	30.7	35.1	32.7	
		$H^5C^1O^2$	108.6	106.7	101.4	
		$H^6C^1O^2$	119.7	120.5	113.8	
		$H^3O^2C^1H^4$	162.7	166.4	162.9	
33	C_1	C^1C^2	1.306	1.401	1.342	n
		C^2O^3	1.213	1.188	1.197	
		C^1H^4	1.592	1.597	1.634	
		C^2H^4	1.249	1.237	1.194	
		C^1H^5	1.049	1.101	1.078	
		$C^1C^2O^3$	156.0	156.1	154.2	
		$H^5C^1C^2$	173.2	112.4	122.0	
		$H^4C^2C^1O^3$	180.0	151.8	166.5	
		$H^5C^1C^2O^3$	180.0	118.4	113.6	
34	C_1	C^1C^2	1.424	1.422	1.349	n
		C^1O^3	1.391	1.360	1.376	
		C^2O^3	1.446	1.457	1.783	
		C^1H^4	1.454	1.454	1.327	
		C^2H^4	1.354	1.354	1.385	
		C^1H^5	1.082	1.082	1.063	
		$H^5C^1C^2$	166.9	167.7	146.1	
		$H^4C^1C^2O^3$	113.8	113.2	108.7	
		$H^5C^1C^2O^3$	-149.9	-155.2	-162.3	
35	C_1	C^1C^2	1.333	1.322	1.280	n
		C^1O^3	1.913	1.924	1.918	
		C^2O^3	1.286	1.272	1.347	
		C^2H^4	1.086	1.098	1.065	
		C^1H^5	1.053	1.064	1.053	
		$C^1C^2O^3$	93.8	95.8	93.8	
		$H^4C^2C^1$	137.6	134.2	138.6	
		$H^5C^1C^2$	168.0	164.6	167.2	
		$H^4C^2C^1O^3$	180.0	180.0	178.1	
		$H^5C^1C^2O^3$	0.0	0.0	51.4	
36	C_1	C^1C^2	1.247	1.241	1.218	n
		C^2O^3	1.312	1.299	1.364	
		C^2H^4	1.206	1.194	1.151	
		O^3H^4	1.488	1.525	1.466	
		C^1H^5	1.050	1.061	1.052	
		$C^1C^2O^3$	150.0	148.8	166.0	
		$H^5C^1C^2$	167.1	159.6	172.5	
		$H^4C^2C^1O^3$	180.0	180.0	178.9	
		$H^5C^1C^2O^3$	180.0	180.0	174.2	
37	C_1	C^1C^2	1.499	1.521	1.479	n
		C^1O^3	1.899	1.854	1.827	
		C^2O^3	1.276	1.258	1.350	
		C^1H^4	1.403	1.377	1.360	
		O^3H^4	1.239	1.227	1.239	
		C^1H^5	1.091	1.104	1.087	
		$C^1C^2O^3$	86.0	83.1	80.3	

Table I (Continued)

system	point group	variable[b,c]	MNDO	MNDOC	ab initio[d,e]	ref
37	C_1	$H^4C^1C^2$	82.4	83.6	87.7	n
		$H^5C^1C^2$	119.1	111.4	110.9	
		$H^4C^1C^2O^3$	6.3	4.6	13.7	
		$H^5C^1C^2O^3$	−108.4	−105.8	−99.3	
38	C_s	C^1C^2	1.333	1.327	1.287	n
		C^1O^3	1.771	1.776	1.856	
		C^2O^3	1.378	1.350	1.449	
		C^1H^4	1.275	1.238	1.245	
		O^3H^4	1.303	1.375	1.412	
		C^2H^5	1.070	1.078	1.055	
		$C^1C^2O^3$	81.6	83.1	85.2	
		$H^4C^1C^2$	97.6	99.5	100.6	
		$H^5C^2C^1$	151.2	148.2	148.1	
39	C_1	C^1C^2	1.288	1.282	1.258	n
		C^2O^3	1.314	1.311	1.312	
		O^3H^4	0.955	0.942	0.955	
		C^1H^5	1.413	1.431	1.314	
		C^2H^5	1.322	1.277	1.303	
		$C^1C^2O^3$	163.4	164.8	170.0	
		$H^4O^3C^2$	111.1	109.3	115.7	
		$H^5C^1C^2$	58.4	55.8	60.8	
		$H^4O^3C^2C^1$	110.4	112.3	102.2	
		$H^5C^1C^2O^3$	−160.5	−157.6	−164.0	
41	C_2	C^1C^2	1.424	1.416	1.401	o
		C^1H^4	1.457	1.432	1.532	
		C^2H^4	1.859	1.845	1.839	
		C^2H^5	1.078	1.082	1.076	
		C^1H^6	1.094	1.096	1.079	
		C^1H^7	1.100	1.100	1.076	
		$C^1C^2C^3$	101.2	100.0	108.9	
		$H^6C^1C^2$	121.4	121.4	122.4	
		$H^7C^1C^2$	120.9	120.0	116.9	
		$H^6C^1C^2C^3$	−133.4	−137.5	−146.5	
		$H^7C^1C^2C^3$	77.3	77.6	68.3	
43	C_{2v}	O^1C^2	1.294	1.282	1.269	o
		O^1H^4	1.318	1.307	1.335	
		C^2H^4	1.689	1.661	1.590	
		C^2H^5	1.087	1.095	1.065	
		$O^1C^2O^3$	100.7	101.6	108.5	
45	C_s	C^1C^2	2.110	2.016	2.216	p, q
		C^2O^3	1.174	1.159	1.146	
		C^1O^4	1.213	1.199	1.208	
		C^1H^5	1.599	1.594	1.916	
		C^2H^5	1.108	1.123	1.081	
		C^1H^6	1.112	1.128	1.107	
		$C^1C^2O^3$	112.2	110.9	101.2	
		$C^2C^1O^4$	111.3	114.5	98.6	
		$H^6C^1O^4$	122.5	119.3	121.2	
47	C_{2v}	C^1C^2	1.684	1.703	2.068	p, r
		C^2O^3	1.180	1.163	1.144	
		C^1H^5	1.548	1.470	1.410	
		H^5H^6	0.884	0.922	1.097	
		$C^1C^2O^3$	135.6	140.2	149.6	
		$H^5C^1C^2$	75.0	74.6	69.9	

[a] A complete geometry definition is given for each system, unles noted otherwise. A few of the structures listed have more than one negative eigenvalue of the force constant matrix (e.g., **7**, **45**, **47**; see text). [b] See Figure 1 for geometry definition. [c] Bond length A^iB^j (in Å), bond angle $A^iB^jC^k$ (in deg), dihedral angle $A^iB^jC^kD^l$ (in deg), and angle A^i–$B^jC^kD^l$ (in deg) of A–B with plane BCD. [d] 6-31G* basis for **5–24**, 4-31G basis for **33–43**, 3-21G basis for **45** and **47**. [e] Some of the values given have been computed from the literature data. The sign of some dihedral angles has been switched to conform with out sign convention. [f] Reference 15. [g] Reference 14. [h] Value not given in ref 14. [i] Angle taken from Figure 1 of ref 14 (no unambiguous definition). [j] Reference 16. [k] SDMC4(DZP): C^1O^2 1.183, C^1H^3 1.096, C^1H^4 1.637, H^3H^4 1.301, $H^3C^1O^2$ 162.7, $H^4C^1O^2$ 110.2 (ref 26). [l] The geometry of **23** is defined incompletely in ref 16. [m] M is the midpoint of O^2–H^3. [n] Reference 18. [o] Reference 19. [p] Reference 20. [q] STO-3G: C^1C^2 2.037, C^1H^5 1.662, $C^2C^1O^4$ 108.7 (ref 20). [r] STO-3G: C^1C^2 1.923, H^5H^6 0.981, $C^1C^2O^3$ 144.3 (ref 20).

total energies. The ab initio RHF results in Tables II and III refer to the basis set used in the geometry optimizations, i.e., RHF/6-31G* in Table II and RHF/4-31G in Table III, while the correlated ab initio results, i.e., MP4(SDQ) in Table II and MP3 in Table III, refer to the 6-31G** basis set. Comparison between the last two columns in Table II for systems **1–16** indicates how much high-level correlated ab initio energies (MP4(SDQ)/6-31G**) may change by further theoretical refinements; these changes may be taken as an error estimate for

the best ab initio energies in Table III (MP3/6-31G**). Table IV lists the semiempirical and ab initio activation energies (barrier heights without zero-point corrections) for all reactions defined in Schemes I–V. The activation energies refer to the endothermic reactions so that any errors in the semiempirical results should mainly be associated with the transition states, the energies of the stable educts normally being given reliably.[3,5] Figure 3 shows the correlation between the semiempirical and ab initio activation energies for reactions A–T (see Table IV). Table V compares

Semiempirical and ab Initio Transition States

J. Am. Chem. Soc., Vol. 107, No. 15, 1985 4427

Table II. Relative Energies (kcal/mol)[a] for 1-24

system		MNDO	MNDOC[b]	ab initio results[c]		
				RHF[d]	MP4(SDQ)[e]	BEST[f]
C_2H_4	1	0.0	0.0	0.0	0.0	0.0
	2	73.0	58.9	68.6	78.1	77.9
	3	106.9	86.2	88.8	94.6	93.3[g]
	4	43.7	40.7	54.6	53.0	47.4
	5	95.1	78.7	82.1	80.7	77.7
	6	124.8	100.4	115.6	104.9	99.7
	7	149.4	140.3	151.8	140.9	133.2
	8	125.4	115.9	129.7	122.6	115.9
	9	138.1	105.2	105.2	101.5	95.5[g]
CH_2O	10	0.0	0.0	0.0	0.0	0.0
	11	46.5	33.6	52.0	54.3	53.2
	12	46.4	32.1	57.7	59.6	58.5[h]
	13	27.5	5.9	1.0	2.8	3.2
	14	108.7	93.3	104.7	91.0	84.7
	15	96.5	71.3	108.5	95.5	85.9[i]
	16	66.9	56.5	80.4	85.5	84.4[h]
	17	155.9	125.5	132.1	j	j
CH_3OH	18	0.0	0.0	0.0	0.0	0.0
	19	25.1	20.3	26.5	26.9	26.1
	20	71.6	53.9	78.5	81.3	81.0
	21	103.9	85.3	95.6	103.9	103.9
	22	135.3	128.6	115.5	103.0	102.5
	23	109.4	91.1	101.7[k]	l	m
	24	101.2	82.7	102.2[k]	95.9	96.1

[a] Not including any corrections for zero-point vibrational energies. [b] MNDOC BWEN at MNDOC SCF geometries. [c] References 14, 36, and 37 for 1-9; ref 15-17 for 10-24. [d] RHF/6-31G* at RHF/6-31G* geometries, except for 23-24.[k] [e] MP4(SDQ)/6-31G** at RHF/6-31G* geometries. [f] Unless noted otherwise: for C_2H_4, MP4(SDQ)/6-31G** at RHF/6-31G* geometries with triple-substitution correlation corrections and triple-basis split corrections; for CH_2O, MP4-(SDTQ)/6-311++G(3df,3pd) at MP2/6-31G* geometries; for CH_3-OH, MP4(SDQ)/6-31G** at MP2/6-31G* geometries. [g] MP4-(SDTQ)/6-311G** at MP2/6-31G* geometries, energies relative to 4. [h] Derived from column MP4(SDQ), energies relative to 11. [i] Reference 26 gives 86.0 ± 2.5 kcal/mol. [j] No correlated value available. [k] RHF/6-31G** at RHF/6-31G* geometries, energy for 23 (24) relative to 21 (20). [l] The MP4(SDQ) energy of 23 lies below that of 21. [m] No transition structure was found at the MP2/6-31G* level.

Table III. Relative Energies (kcal/mol)[a] for 25-39

system		MNDO	MNDOC[b]	ab initio results[c]	
				RHF[d]	MP3[e]
C_2H_2O	25	0.0	0.0	0.0	0.0
	26	108.2	76.4	83.0	90.1
	27	70.6	64.5	76.8	84.2
	28	65.5	55.3	78.9	58.8
	29	62.4	75.8	88.5	80.3
	30	86.4	72.3	75.2	83.7
	31	19.0	21.9	31.8	36.0
	32	108.5	76.9		
	33	81.2	83.2	80.5	74.2
	34	141.2	119.2	145.1	121.3
	35	83.1	84.8	94.7	89.3
	36	124.6	105.7	126.3	113.7
	37	164.4	126.5	160.1	138.5
	38	148.1	123.8	141.0	118.6
	39	107.7	78.5	92.2	80.2

[a] Not including any corrections for zero-point vibrational energies. [b] MNDOC BWEN at MNDOC SCF geometries. [c] Reference 18. [d] RHF/4-31G at RHF/4-31G geometries. [e] MP3/6-31G** at RHF/4-31G geometries.

the zero-point vibrational energies at the MNDO and ab initio RHF level which are based on the harmonic vibrational frequencies obtained from force constant analysis. These frequencies are listed in Table VI for the species **10-17** on the CH_2O potential surface.

In the remainder of this section, we shall present the results for the reactions in Schemes I-V. The discussion in the next section will then provide a general evaluation.

Table IV. Activation Energies (kcal/mol)[a]

reaction	MNDO	MNDOC	ab initio	
			RHF	BEST
A	95.1	78.7	82.1	77.9[b]
B	124.8	100.4	115.6	99.7
C	149.4	140.3	151.8	133.2
D	81.7	75.2	75.1	68.5
E	94.4	64.5	50.6	48.1
F	108.7	93.3	104.7	84.7
G	96.5	71.3	108.5	85.9
H	20.4	22.9	28.4	31.2
I	128.4	119.6	131.1	c
J	135.3	128.6	115.5	102.5
K	109.4	91.1	98.3[d]	103.9[b]
L	101.2	82.7	101.5[d]	96.1
M	108.5	76.9	83.0[b]	90.1[b]
N	81.2	83.2	80.5	84.2[b]
O	75.7	63.9	66.2	62.5
P	18.7	9.0	6.2	5.6
Q	85.7	48.0	52.5	38.3
R	105.6	83.8	94.5	77.7
S	145.4	104.6	128.3	102.5
T	88.7	56.6	60.4	47.7[b]
U	95.1	88.5	107.6[e]	92.9[f]
V	68.5	66.6	59.5[e]	44.3[f]
W	95.9	73.7	100.4[g]	c
X	104.4	65.5	76.0[g]	61.6[h]

[a] Based on the data in Tables II and III, unless noted otherwise. Entries in column BEST are obtained from column BEST in Table II and column MP3 in Table III. [b] Endothermicity of reaction, no barrier. [c] No correlated value available. [d] RHF/6-31G** at RHF/6-31G* geometries (ref 16). [e] RHF/4-31G at RHF/4-31G geometries (ref 19). [f] CEPA/DZP at RHF/4-31G geometries (ref 19). [g] RHF/3-21G at RHF/3-21G geometries (ref 20). [h] SDCI/3-21G with Davidson correction at RHF/3-21G geometries (ref 20).

Table V. Zero-Point Vibrational Energies (kcal/mol)

system	MNDO	ab initio SCF[a]	system	MNDO	ab initio SCF[a]
1	33.5	34.4	25	21.6	21.8
2	31.0	31.6	26	14.7	14.8
3	22.9	23.0	27	19.9	19.2
4	25.0	25.1	28	21.9	21.4
5	29.7	30.9	29	21.7	20.5
6	26.1	28.1	30	21.2	20.8
7	25.5	26.7	31	22.1	22.2
8	26.7	27.8	32	16.0	c
9	20.4	21.7[b]	33	18.0	17.9
10	18.0	18.3	34	18.2	17.0
11	17.8	18.2	35	20.0	19.0
12	17.5	17.8	36	17.7	16.9
13	9.5	10.1	37	16.9	16.3
14	13.9	13.9	38	18.6	17.6
15	12.6	12.2	39	18.5	17.4
16	15.6	15.4	40	52.3	c
17	10.8	c	41	49.1	c
18	33.9	34.7	42	22.7	c
19	24.1	24.9	43	19.8	c
20	23.9	24.8	44	25.3	c
21	25.7	25.7	45	21.1	21.1
22	26.8	28.7	46	21.4	c
23	29.2	29.6	47	16.3	17.1
24	27.6	28.8	48	13.0	c

[a] 6-31G* basis for **1-24**, 4-31G basis for **30**, and 3-21G basis for **25-29** and **31-47** (see ref 14, 16, 18). [b] The value for **9** is 1.3 kcal/mol below that for **3** (ref 36). [c] Not available.

Scheme I. The C_2H_4 Surface. The general features of the potential surface are analogous in MNDO, MNDOC, and RHF/6-31G*. All three methods predict four genuine transition states (**5, 6, 8,** and **9**) and one stationary point (**7**) with two negative eigenvalues of the force constant matrix. The optimized MNDOC and RHF/6-31G* geometries for **5-9** are generally quite similar (see Figures 1 and 2 and Table I) except for the $H^6C^1C^2$ angle in **8**. The MNDO geometries sometimes deviate more strongly, e.g., with regard to the angles in **5, 7,** and **8,** but

Table VI. Vibrational Frequencies (cm⁻¹)[a]

system	symmetry	MNDO	ab initio[b]	system	symmetry	MNDO	ab initio[b]
10[c]	a_1	3302	3161	14	a'	3284	3168
		2115	2030			2772	2816
		1490	1680			1839	1649
	b_1	1186	1336			1246	1431
	b_2	3255	3233			3046i	2710i
		1210	1383		a''	500	649
11	a'	3935	4045	15[e]	a'	2933	3263
		3200	3101			2236	2149
		1702	1647			1824	1306
		1494	1446			892	755
		1146	1333			2539i	2184i
	a''	963	1128		a''	944	1056
12	a'	3792	3985	16	a	4011	4070
		3159	2992			3063	2977
		1713	1611			1612	1524
		1385	1450			1313	1281
		1165	1370			921	890
	a''	1014	1041			1316i	1364i
13[d]	σ_g	4294	4643	17	a'	2337	f
	σ	2383	2439			1859	
						1764	
						711	
						5079i	
					a''	773	

[a] The transition states **14–17** have one imaginary frequency. [b] RHF/6-31G* values from ref 16. For other ab initio values see ref 17, 23, 24, and 26. [c] Harmonized experimental frequencies: a_1 2978, 1778, 1529; b_1 1191; b_2 2997, 1299 (ref 45). [d] $\sigma_g(\sigma)$ refers to H_2 (CO). [e] MC10(DZP): a' 3207, 1815, 1282, 791, 1853i; a'' 849 (ref 26). [f] Not available.
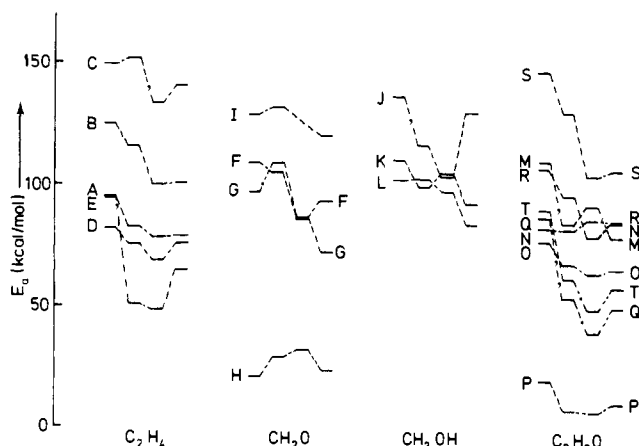
Figure 3. Correlations between calculated activation energies, as given numerically in Table IV. From left to right, the activation energies are always drawn in the order: MNDO–ab initio RHF–ab initio BEST–MNDOC.

still resemble the RHF/6-31G* structures qualitatively. The best correlated ab initio energies are reproduced much better by MNDOC than by MNDO (see Table II). The MNDOC activation energies are in the same sequence as the ab initio ones, with fairly small quantitative discrepancies (see Figure 3). The major shortcoming of the semiempirical predictions concerns the intermediates **2** and **3**. In the best correlated ab initio treatments, there is no potential well for ethylidene **2**[14] and a very shallow one for vinylidene **3**,[36,37] whereas MNDO and MNDOC (like ab initio RHF[14,36–38]) predict them to be stable minima, with appreciable barriers for the rearrangements **2** → **1** and **3** → **4**. MNDO, MNDOC, and the ab initio RHF treatment thus substantially overestimate the barriers for these [1,2]-hydrogen shifts.

With regard to the conversion of ethylene to acetylene, Scheme I offers three mechanistic alternatives. The direct 1,2 elimination of hydrogen is ruled out by all computational methods. The two-step pathway via **5** and **8** is favored by MNDO (incorrectly),

(36) Krishnan, R.; Frisch, M. J.; Pople, J. A.; Schleyer, P. v. R. *Chem. Phys. Lett.* **1981**, *79*, 408.
(37) Pople, J. A. *Pure Appl. Chem.* **1983**, *55*, 343.
(38) Schaefer, H. F., III *Acc. Chem. Res.* **1979**, *12*, 289.

while MNDOC and the ab initio treatments predict a two-step mechanism via vinylidene, i.e., a 1,1 elimination of hydrogen via **6** followed by a [1,2]-hydrogen shift via **9**.

Scheme II. The CH₂O Surface. All methods studied produce four genuine transition states (**14–17**) with remarkably similar geometries (see Figures 1 and 2 and Table I). The lowest activation energy is always associated with the internal rotation (H) in hydroxycarbene via **16** and the highest one with the 1,2 addition (I) of H_2 and CO via **17** (see Figure 3 and Table IV). The best correlated ab initio calculations[17] predict the activation energies for the [1,2]-hydrogen shift (F) and the 1,1 elimination (G) in formaldehyde to be almost equal, whereas MNDO and MNDOC give a higher activation energy for F which is partly due to their tendency to overestimate the barriers to [1,2]-hydrogen shifts (see above).

Table VI compares harmonic vibrational frequencies at the MNDO and RHF/6-31G* level. Deviations between calculated frequencies are of the order of 10% for the transition states **14–16** and slightly smaller (typically 7%) for the minima **10–13**. Since these deviations occur in both directions, the calculated zero-point vibrational energies for **10–16** show excellent agreement (see Table V), with mean absolute deviations of 2% (0.4 kcal/mol) between MNDO and RHF/6-31G* results. This type of agreement is also found for other systems (see Table V).

The 1,1 elimination (G) of hydrogen from formaldehyde has recently been studied by extensive ab initio MCSCF-CI calculations.[26] The final barrier height of 86.0 ± 2.5 kcal/mol agrees with the best ab initio value[17] of 85.9 kcal/mol included in Tables II and IV. With regard to transition-state geometries and frequencies, however, the new results[26] often differ appreciably from previous ones[16,23] (see best new data for **15** in footnote *k* of Table I and footnote *e* of Table VI). These differences provide a rough measure of the uncertainties which may be expected for all ab initio reference data in Tables I and VI.

Scheme III. The CH₃OH Surface. Three unimolecular decompositions of methanol are studied. For the 1,2 elimination (J) and the 1,1 elimination (L) of hydrogen, all methods predict genuine transition states (**22** and **24**) with similar geometries (see Figure 1 and Table I). The 1,1 elimination is always favored, being the lowest of all three decomposition pathways according to MNDO, MNDOC, and the best correlated ab initio treatment (see Figure 3 and Table IV).

The third decomposition (K) of methanol leads to the formation of singlet methylene and water, the reverse reaction being a

carbene insertion. The published[16] RHF/6-31G* transition structure **23** for this reaction resembles optimized MNDO and MNDOC structures (see Table I) with two negative eigenvalues of the force constant matrix. The genuine MNDO and MNDOC transition states (energies see Table II) represent only a weak interaction between singlet methylene and water (compare, e.g., the optimized MNDO (MNDOC) values C^1O^2 2.152 (2.124) Å and C^1H^3 2.425 (2.388) Å with the values in Table I). Hence, the semiempirical and the ab initio SCF transition structures for this carbene insertion are qualitatively different. The MNDO and MNDOC barriers for the insertion are fortuitously close to the RHF/6-31G* value (5.5 and 5.8 vs. 6.1 kcal/mol; see **21** and **23** in Table II); however, at the best correlated ab initio level, the barrier disappears completely,[16] so that the semiempirical results for this reaction must be regarded as misleading.

Scheme IV. The C_2H_2O Surface. The potential surface of ketene is the most complicated one presently studied since the ab initio reference calculations[18] involve seven minima (**25-31**) and seven transition states (**33-39**). All these minima and transition states are also found in MNDO and MNDOC calculations. For the conversion **26 → 25**, there is apparently no barrier at the ab initio level,[18] whereas MNDO and MNDOC give a very small barrier (0.3 and 0.5 kcal/mol, respectively); the corresponding C_s transition state **32** is characterized in MNDO (MNDOC) by the data CC 2.753 (2.783) Å, OCC 169.1° (167.9°), and C–CH$_2$ 89.2° (91.1°).

The calculated MNDO, MNDOC, and RHF/4-31G[18] transition structures **33-39** are generally in satisfactory qualitative agreement, but some more specific comments seem appropriate (see Figure 1 and Table I). For **33**, the MNDO and ab initio geometries are fairly similar, whereas MNDO deviates appreciably with regard to the position of the (nonreactive) atom H^5 bonded to the carbenoid center C^1 (see angles involving H^5). For **34**, MNDO and MNDOC underestimate the length of the breaking C^2O^3 bond. For **35**, the MNDO and the MNDOC transition structures are planar in contrast to the ab initio one; however, this discrepancy is not too serious because the potential surface is quite flat with respect to nonplanar deformations; in fact, optimizations starting from the RHF/4-31G structure of **35** converge to nonplanar MNDO and MNDOC structures under the default criteria of our program and produce the planar structures only when using more stringent convergence criteria. For **36**, analogous remarks apply as for **35**; here, however, the deviations from planarity in the ab initio structure are extremely small, anyway. For **37-39**, MNDO, MNDOC, and RHF/4-31G* predict transition structures of remarkable similarity (see also Figure 2). This is particularly gratifying for structures **37** and **38** which correspond to rather complicated rearrangements, i.e., concomitant ring openings and hydrogen shifts.

With regard to relative energies (Table III) and activation energies (Figure 3 and Table IV), the best ab initio results (MP3/6-31G**) are reproduced more closely by MNDOC than by MNDO. All methods predict ketene **25** to be the most stable isomer on the surface followed by hydroxyacetylene **31**, but only MNDOC and MP3/6-31G** put oxiranylidene **28** in third place, significantly below the other isomers. Both MNDOC and the ab initio treatments predict the same sequence of activation energies (except for reactions M, and N, R, see Figure 3), the quantitative discrepancies between the MNDOC and MP3/6-31G** values being normally fairly small; as usual, however, MNDOC tends to overestimate the barriers to [1,2]-hydrogen shifts (see reactions R and T in Figure 3).

The semiempirical calculations arrive at a number of qualitative conclusions which are the same as in the previous ab initio study:[18] Hydroxyacetylene **31** is predicted to be a potentially observable isomer, the rate of its conversion to ketene **25** being determined by the barrier to the initial [1,2]-hydrogen shift via **36** (see reaction R in Figure 3). Oxiranylidene **28** is also expected to be observable since there seems to be no path to ketene with a very low activation energy. On the other hand, oxirene **29** is found to rearrange easily to ketene, the rate-determining step being the ring opening via **35** (see reaction P in Figure 3).

The major discrepancy in the qualitative conclusions concerns formyl-methylene **27** and hydroxyvinylidene **30**. These isomers turn out to be unstable at the best correlated ab initio level since the barriers for the rearrangements via **33** and **39** vanish. MNDO and MNDOC as well as the ab initio RHF/4-31G approach incorrectly predict potential wells for **27** and **30** (analogous to the case of ethylidene **2**; see above).

Scheme V. Other Reactions. The transition structures **41** and **43** for the [1,3]-hydrogen shifts in propene and formic acid belong to the point groups C_2 and C_{2v}, respectively, the symmetry being derived from the fact that these antarafacial shifts are narcissistic reactions.[39] The optimized geometries of **41** and **43** are quite similar at the MNDO, MNDOC, and RHF/4-31G[19] levels (see Figures 1 and 2 and Table I). The semiempirical activation energies (see Table IV) are close to the best ab initio value in the case of propene (reaction U) but too high in the case of formic acid (reaction V).

The last two reactions in Scheme V represent unusual unimolecular decompositions of *cis*-glyoxal leading to formaldehyde and carbonmonoxide (reaction W via **45**) or to hydrogen and two carbonmonoxide molecules (reaction X via **47**). Both in the ab initio reference calculations[20] and in the present semiempirical study, the geometry optimizations for **45** and **47** were constrained to C_s and C_{2v} symmetry, respectively. Therefore, the resulting structures usually do not correspond to genuine transition states, as can be seen from the number of negative eigenvalues of the force constant matrix for **45** (**47**): MNDO, MNDOC, and RHF/STO-3G 2 (3), RHF/3-21G 1 (1), RHF/DZ and RHF/DZP (2).[20] The qualitative features of the optimized stationary points **45** and **47** are the same in MNDO, MNDOC, and the ab initio RHF treatments[20] (see Figures 1 and 2 and Table I for a comparison with RHF/3-21G[20]) although MNDO and MNDOC underestimate the length of the breaking CC bond. Quantitatively, the MNDO and MNDOC geometries for **45** and **47** are closest to those obtained from RHF/STO-3G (see footnotes *q* and *r* in Table I). With regard to activation energies (see Table IV), no correlated ab initio value is available for reaction W so that the MNDOC value is probably the most reliable one. For reaction X, MNDOC and the best correlated ab initio treatment yield similar estimates for the barrier. Since the optimized structures for **45** and **47** do not qualify as genuine transition states (see above), the "true" MNDO and MNDOC activation energies for reactions W and X are expected to be somewhat lower than listed in Table IV. Moreover, the zero-point correlations will reduce the effective semiempirical barriers further, by about 4 kcal/mol for W and 9 kcal/mol for X (see Table V) so that the effective MNDOC barriers should be slightly below 70 kcal/mol for W and 57 kcal/mol for X. These MNDOC predictions are compatible with recent experimental evidence:[40,41] A photochemical molecular beam study finds both dissociation channels W and X to be open at an excitation energy of 65 kcal/mol,[40] and a thermal shock-wave study shows channel X to be predominant, with an observed barrier of 55.1 kcal/mol.[41]

5. Discussion

Having presented our results in detail, we now address the general question of whether semiempirical methods such as MNDO and MNDOC can give useful and reliable information on transition states in chemical reactions.

For all systems studied, the qualitative features of the potential surfaces are predicted by MNDO and MNDOC in complete analogy to the ab initio RHF treatments. The same types of minima and transition states are found, the only major exception being the carbene insertion reaction via **23** (see above). When comparing with the best correlated ab initio treatments, MNDO, MNDOC, and ab initio RHF share one particular qualitative deficiency in that they predict significant potential wells for

(39) Salem, L. *Acc. Chem. Res.* **1971**, *4*, 322.
(40) Hepburn, J. W.; Buss, R. J.; Butler, L. J.; Lee, Y. T. *J. Phys. Chem.* **1983**, *87*, 3638.
(41) Saito, K.; Kakumoto, T.; Murakami, I. *J. Phys. Chem.* **1984**, *88*, 1182.

Table VII. Statistical Evaluation of Transition-State Predictions[a]

property	N[b]	mean absolute deviation		ab initio reference
		MNDO	MNDOC	
bond length, Å	112	0.057	0.056	RHF
active[c]	70	0.078	0.073	RHF
passive[c]	42	0.018	0.025	RHF
bond angle, deg	58	7.9	6.2	RHF
dihedral angle, deg	20	11.6	7.9	RHF
activation energy, kcal/mol	24	13.6	11.2	RHF
	22	21.9	8.7	BEST

[a] MNDO and MNDOC vs. ab initio data given in Tables I and IV. [b] Number of comparisons. [c] "Active" bonds are broken or formed in the reaction; "passive" bonds remain formally unchanged.

carbenoid species such as **2, 3, 27,** and **30** which disappear at higher theoretical levels. Hence, MNDO and MNDOC seem to be suitable for fast initial scans of potential surfaces to assess their qualitative features, but it has to be kept in mind that some of these characteristics may change at higher levels.

With regard to the accuracy of semiempirical transition structures, Table VII gives a statistical evaluation of the comparisons with ab initio RHF data in Table I. Apparently, MNDOC reproduces the ab initio RHF transition structures slightly better than MNDO,[42] the mean absolute deviations being of the order of 0.07 (0.03) Å for the bond lengths of "active" ("passive") bonds, 6° for bond angles, and 8° for dihedral angles. Furthermore, in the majority of cases, the MNDOC transition structures are similar to the ab initio RHF ones in the sense that every single deviation in bond lengths and in angles is below 0.1 Å and 10°, respectively (see Table I). Based on this satisfactory agreement, we may draw two conclusions: First, for large molecules where ab initio calculations might be impossible, we expect semiempirical transition structures to be reliable enough to form the basis of qualitative arguments, e.g., concerning stereochemical problems. Second, for computational studies of medium-size molecules, it seems advantageous to combine semiempirical and ab initio calculations in the following manner: Semiempirical methods can be used efficiently for a fast initial determination of transition structures which can then serve as starting points for automatic ab initio optimizations; this suggestion is supported by the success that we enjoyed with the reverse procedure (see section 3).

The MNDO vibrational frequencies for transition states are normally reasonably close to the corresponding ab initio RHF values (see Table VI) so that it might be recommended to use them in RRKM calculations for large molecules.[10] With respect to zero-point vibrational energies, there is generally excellent agreement between MNDO and ab initio RHF (see Table V), the mean absolute deviation being 0.7 kcal/mol (3%) in 39 comparisons; the MNDO values tend to be slightly lower than those from RHF/6-31G* and slightly higher than those from RHF/3-21G (see Table V). Hence, zero-point vibrational corrections to potential barriers can safely be deduced from semiempirical MNDO-type calculations.

Knowing the geometries and the vibrational frequencies of reactants and transitions states, the techniques of statistical thermodynamics may be used to compute activation entropies and kinetic isotope effects.[43,44] Based on the satisfactory agreement between semiempirical and ab initio transition-state geometries and frequencies (see above), we expect activation entropies and kinetic isotope effects to be predicted reasonably well by semi-

empirical methods. MNDO applications of this kind have indeed been quite successful in several mechanistic studies.[9,10,44] Such applications receive additional support from our present comparisons.

Turning to activation energies, the situation appears to be less favorable. Some general trends are obvious from Figure 3 and Table IV: Explicit inclusion of electron correlation normally lowers the calculated activation energies both in semiempirical methods (i.e., MNDO > MNDOC) and in ab initio treatments (i.e., RHF > BEST). Likewise, ab initio activation energies tend to be somewhat smaller than the corresponding semiempirical ones (i.e., MNDO > RHF and MNDOC > BEST in most cases). For a given potential surface, the sequence of activation energies is roughly the same for the different approaches, particularly for MNDOC vs. BEST, although crossings in the correlations do occur (see Figure 3). Table VII evaluates the MNDO and MNDOC predictions for activation energies on a statistical basis: Both methods perform similarly with respect to the ab initio RHF results, but MNDOC is far superior when compared to the best correlated ab initio data, the mean absolute deviations being 21.9 kcal/mol for MNDO and 8.7 kcal/mol for MNDOC; the corresponding value for ab initio RHF is 11.2 kcal/mol (see Table IV).

Hence, if we accept the best correlated ab initio results as reliable reference data, MNDOC turns out to be more suitable than MNDO for quantitative estimates of activation energies. This is probably partly due to the explicit inclusion of electron correlation in the MNDOC formalism.[5] On the other hand, it should also be pointed out that many reactions studied presently involve carbonmonoxide and carbenes, i.e., systems which are known to be problematic for MNDO (not for MNDOC).[3,5,35] Therefore, we would generally expect MNDO to approach MNDOC in its predictions more closely when dealing with other systems.

In practical applications to large molecules where ab initio calculations might not be feasible, it is often desirable to distinguish between different mechanistic alternatives on the basis of calculated semiempirical activation energies. The preceding results suggest some caution in such an endeavour even though it is often easier to compute relative rather than absolute activation energies (see Figure 3). In our opinion, the semiempirical predictions would seem reliable if the calculated barriers for different pathways differ by large amounts (e.g., larger than the deviations listed in Table VII) or if there are independent error estimates available (e.g., from experience with related reactions). Mechanistic results based on calculated activation energies should preferably be supported by additional evidence derived from transition-state geometries and frequencies (e.g., activation entropies, kinetic isotope effects, stereochemistry, etc.) and by arguments based on the electronic structure of the transition state (e.g., concerning solvent and substituent effects). When applied in such a comprehensive manner, semiempirical calculations are expected to be a valuable tool for studying chemical reactions of large molecules.

6. Conclusion

MNDO and MNDOC usually reproduce the qualitative features of ab initio potential surfaces and transition structures. The calculated semiempirical activation energies are sometimes less accurate than desirable; however, the MNDOC barriers are normally realistic enough to allow correct mechanistic conclusions. The overall agreement between the semiempirical and the ab initio results supports MNDO and MNDOC calculations of transition states for thermal organic reactions, i.e., applications in an area not included in the parametrization of these methods.

(42) For two additional examples, see ref 35 and: Breulet, J.; Schaefer, H. F., III. *J. Am. Chem. Soc.* **1984,** *106,* 1221.
(43) Dewar, M. J. S.; Ford, G. P. *J. Am. Chem. Soc.* **1977,** *99,* 7822.
(44) Brown, S. B.; Dewar, M. J. S.; Ford, G. P.; Nelson, D. J.; Rzepa, H. S. *J. Am. Chem. Soc.* **1978,** *100,* 7832.
(45) Reisner, D. E.; Field, R. W.; Kinsey, J. L.; Dai, H. L. *J. Chem. Phys.* **1984,** *80,* 5968.